HfB2-doped ZrB2-30 vol.% SiC composites: Oxidation resistance behavior

Ebrahim Dodi
Karaj Islamic Azad University Faculty of Sciences
Zohre Balak (Zbalak1983@gmail.com)
Karaj Islamic Azad University Faculty of Sciences https://orcid.org/0000-0003-4232-1462

Research Article

Keywords: ZrB2-30 vol% SiC, Oxidation, HfB2, SPS

Posted Date: April 14th, 2020

DOI: https://doi.org/10.21203/rs.3.rs-21449/v1

Version of Record: A version of this preprint was published on January 22nd, 2021. See the published version at https://doi.org/10.1088/2053-1591/abdf1a.

HfB2-doped ZrB2-30 vol.% SiC composites : Oxidation resistance behavior

Ebrahim Dodi[1], Zohre Balak[*1]

Department of Materials Science and Engineering, Ahvaz Branch, Islamic Azad University, Ahvaz, Iran.

Corresponding Author: Zohre Balak, zbalak1983@gmail.com

Abstract:

In order to investigate the HfB_2 on microstructure and oxidation resistance of ZrB_2-30 vol% SiC, ZrB_2-30 vol% SiC composites with different amount of HfB_2 (4, 8 and 12 vol%) were SPSed. Microstructural evaluations were done by scanning electron microscopic (SEM). In order to investigate the oxidation resistance, the samples were placed in box furnace at the temperature of 1400 C for different times. The samples were weighted before and after the oxidation and the Δw was applied as criterion of oxidation. Thickness of SiO_2 layer and Si depleted layer were also used as oxidation criterion. The results showed that HfB_2 addition, caused to decrease Δw and better oxidation resistance.

Keywords : ZrB_2-30 vol% SiC, Oxidation, HfB_2, SPS

1. Introduction

Due to the growing tendency for high-temperature oxidation resistance materials for several structural and aerospace applications, ultra-high temperature ceramics (UHTCs) have been in the center of attention during last recent years. UHTCs which are known as materials with melting point above 3000 °K, seem to be potential candidates for military and aerospace applications, e.g. nozzle inputs for rockets, air injection combustion systems, missile heads and supersonic vehicles [1-3]. Historically, to reduce the aerodynamic friction-derived heat in primary aerospace vehicles, high radios and thickness components were designed. Also such a design may minimize the generated heat, but challenges the achievable velocity of the vehicles. Therefore, sharp leading edges have been used in new generation of aerospace components which can improve the lift/drag ratio and consequently, overall efficiency of the vehicle. Anyway, such designs can result in higher friction-derived heat input and promote high-temperature reactions at the sharp leading edges. Hence, successful design of leading edges depends on the available high-temperature materials, e.g. UHTCs[3].

Among UHTCs, borides of transition metals (TMBs) such as ZrB2 and HfB2 present unique combinations of mechanical, physical and chemical properties, such as high melting points (>3000°C), high electrical and thermal conductivities, chemical inertness as well as favorable thermal shock resistance. Therefore, although transition metal carbides (TMCs) commonly show higher melting points, TMBs seem to be promising candidates for high-temperature thermomechanical and structural applications [4-10].

Due to its lower density, ZrB2 is the highest studied TMB and several brilliant research works have been carried out on densification, properties and applications of this material [11-13]. The surface of ZrB2 particles are naturally covered by a mixture of low-melting point boron oxide (B2O3) and ZrO2 which challenge its densification and sintering, as well as high temperature oxidation behavior. Encountering high-temperature oxidative environment, B2O3 surface impurity evaporates and leaves a non-protective porous ZrO2 layer remains on ZrB2 surface, which cannot effectively control the oxidation of ZrB2 particles. It has been repeatedly reported that the addition of silicon carbide (SiC) to ZrB2 can promote the formation of borosilicate glassy layer and consequently, improve the oxidation behavior of the material l[1-3, 14-18]. Therefore, numerous research projects have been dedicated to ZrB2-SiC composites through last decades. All at all, there are still several challenges in densification and increased oxidation behavior of ZrB2-SiC composites. Researches indicated the positive influence of additives and sintering aids on the oxidation of the mentioned composites, as well as its densification and sintering behavior.

Among several sintering additives, it has been revealed that HfB2 (melting point: 3380°C) as another member of HUTCs family, not only improves the mechanical properties and thermal shock resistance of ZrB2-SiC composites, but also can influence the oxidation behavior of the composite, as it forms a protective oxide layer, HfO2[5, 7-9]. Anyway, to the best of our understanding, there is no comprehensive report on the effects of HfB2 on oxidation resistance of ZrB2-SiC composites. Therefore, the present study is dedicated to the role of HfB2 in oxidation behavior of ZrB2-SiC-HfB2 ternary composites.

2. Experimental

Commercially pure ZrB2, SiC and HfB2 powders were used as the starting materials. The characteristics of the used materials and their weighting ratio as well as sintering conditions are presented in Tables 1 and 2.

Table 1. Characteristics of the used materials.

Powder	Particle size	Supplier
ZrB_2	20 µm	Northwest Institute for Non-Ferrous Metal Research, China, 99.5% purity
SiC	15 µm	Northwest Institute for Non-Ferrous Metal Research, China, 98.7% purity
HfB_2	20 µm	Northwest Institute for Non-Ferrous Metal Research, China, 98.7% purity

Table 2. Weighting ratio of initial powder as well as sintering conditions.

Sample Code	HfB_2 content Vol%	Temperature ^oC	Time min	Pressure MPa
2	8	1725	4	20
5	8	1725	9	20
6	8	1725	14	20
8	8	1800	9	30
9	12	1800	9	30
11	4	1800	9	30
12	12	1650	9	30
14	12	1725	9	30
17	8	1725	9	30
19	8	1725	9	40

The powders were then weighed and consequently ball-milled using WC balls through ethanol as milling media in a tungsten carbide cup. The milling process was carried out at 250 rpm for 3 hr. Consequently, the milled powder mixture was dried via a heater/stirrer at 160-200 °C and loaded into a graphite die covered with 0.1mm thick graphite foil. The spark plasma sintering process was then carried out via SPS furnace (SPS-20T-10: china) at 1800°C for 9 minutes under the applied pressure of 30MPa. Detailed SPS parameters are presented in Table. 2. To remove the remained graphite foil, the obtained disk-shaped samples were grinded and then, wire cut to achieve 2×4×10 mm beam-shaped samples for oxidation test. The oxidation test was performed in a box furnace at 1400°C for 1, 2, 3, 6, 7, 15, 17 1nd 20 hrs. The weight change was then measured as oxidation progress criterion, based on the following equation:

$$\Delta W_{C-O}\,\% = \frac{W_i - W_a}{W_i} \times 100 \qquad (1)$$

In which, W_{C-O} shows the percentage of weight change due to oxidation, and W_i and W_a show initial and after oxidation weights of the samples, respectively.

3. Results and Discussion

3.1. Microstructural investigations

The average grain size of 4, 8 and 12 vol% HfB2-contained ZrB2-SiC composites, analyzed via Image Tools software, are presented in Table 3. The table also includes measured relative density and open porosity fraction of the samples. Phase analysis was also carried out via Energy Dispersive Spectroscopy (EDS) in both point and map modes, and presented in Figures 1 and 2. These images confirms the formation of (Zr, Hf)B2 solid solution (bright gray phases) together between SiC (dark) and ZrB2 (dark gray) grains, which is adjusted by previously published reports [5, 7-9].

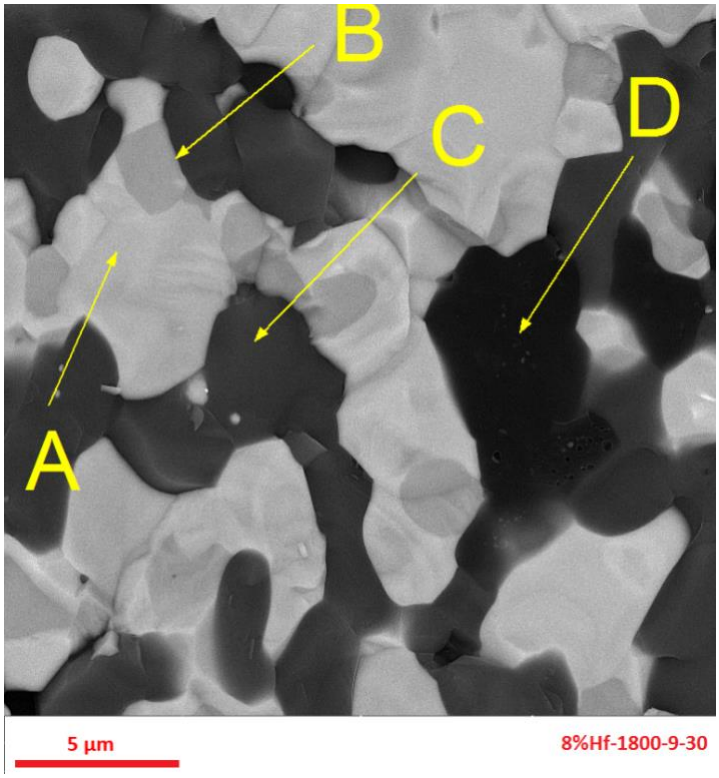

Fig. 1. Point analysis of ZrB_2-30SiC-8HfB_2 SPSed at the condition of 1800, 9 min, 30 MPa.

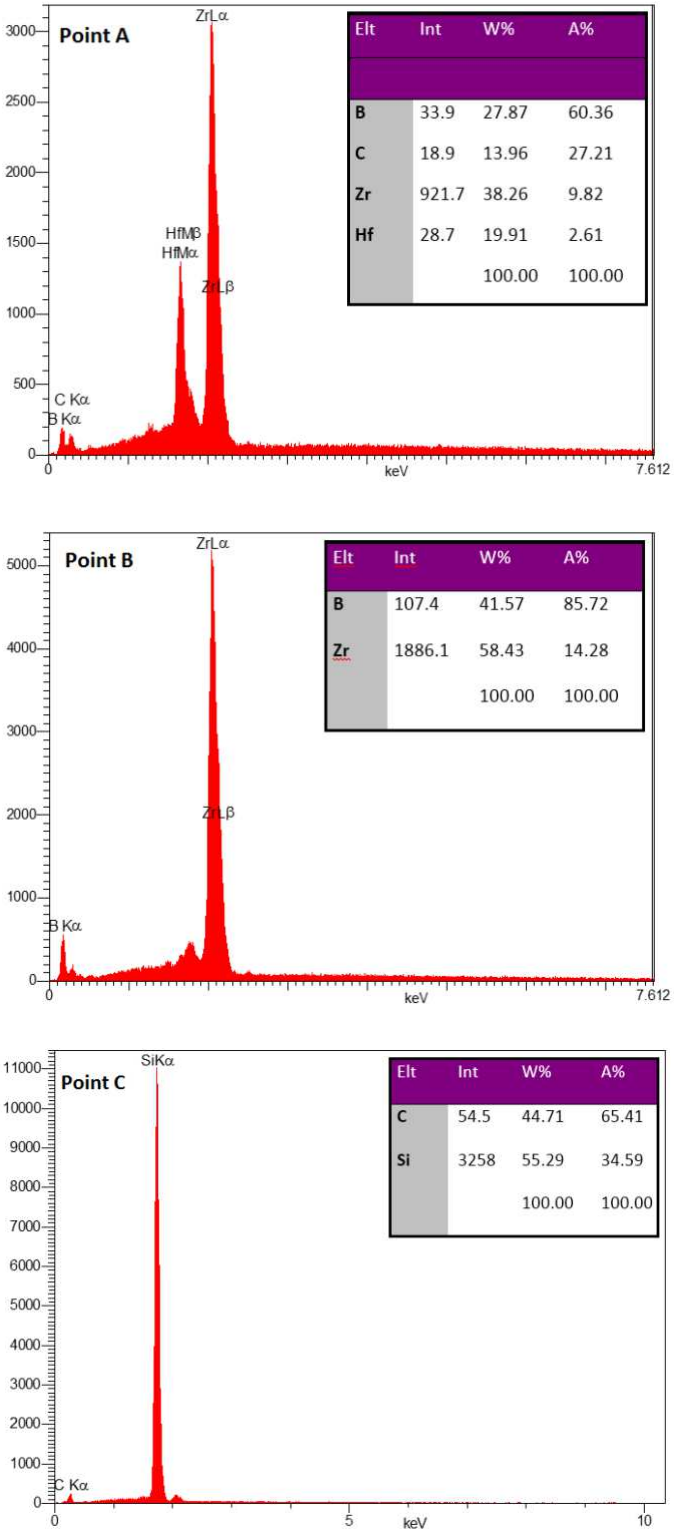

Continue Fig. 1. Point analysis of ZrB_2-30SiC-8HfB_2 SPSed at the condition of 1800, 9 min, 30 MPa

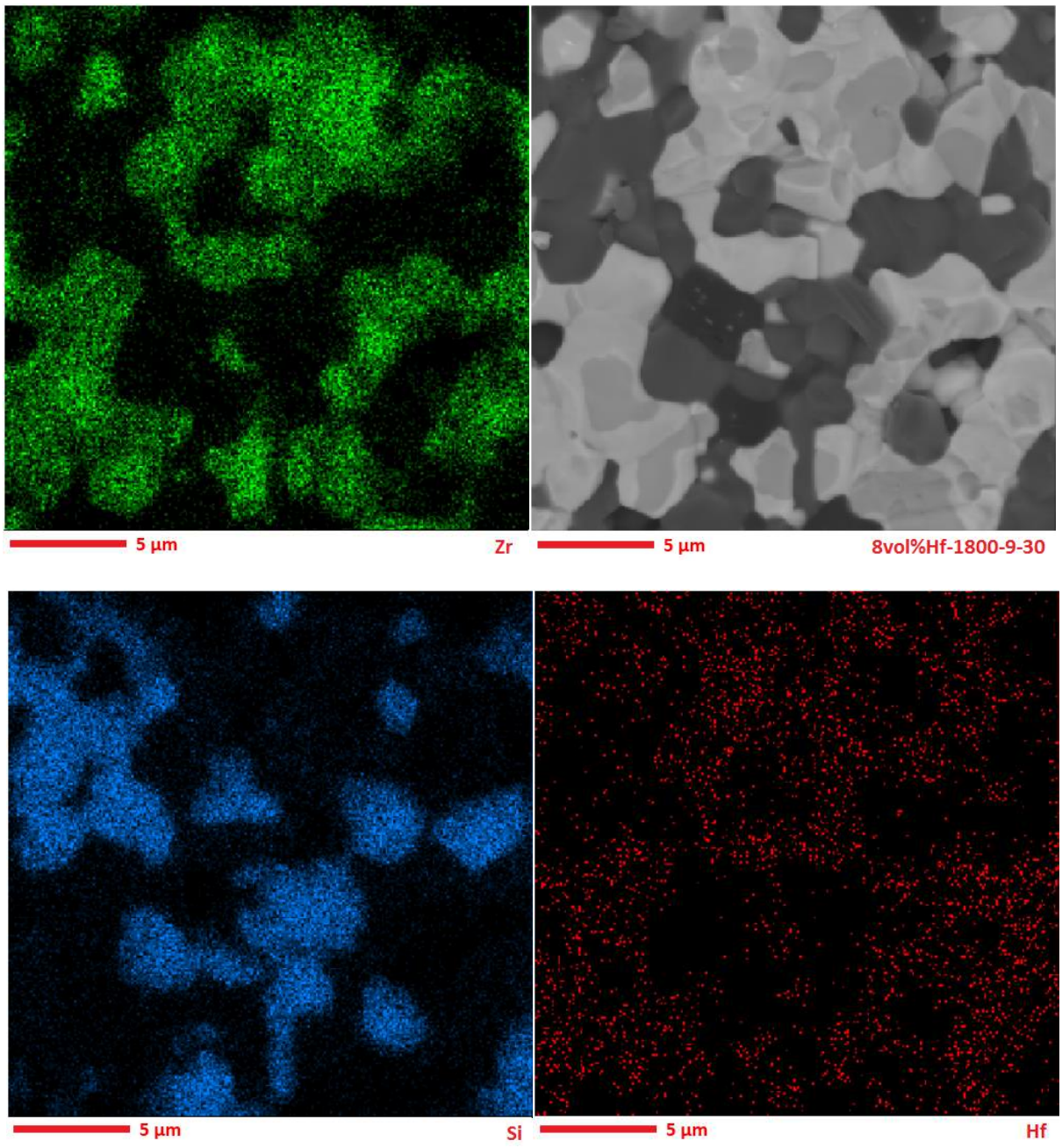

Fig. 2. Map analysis of ZrB_2-30SiC-8HfB_2 SPSed at the condition of 1800, 9 min, 30 MPa

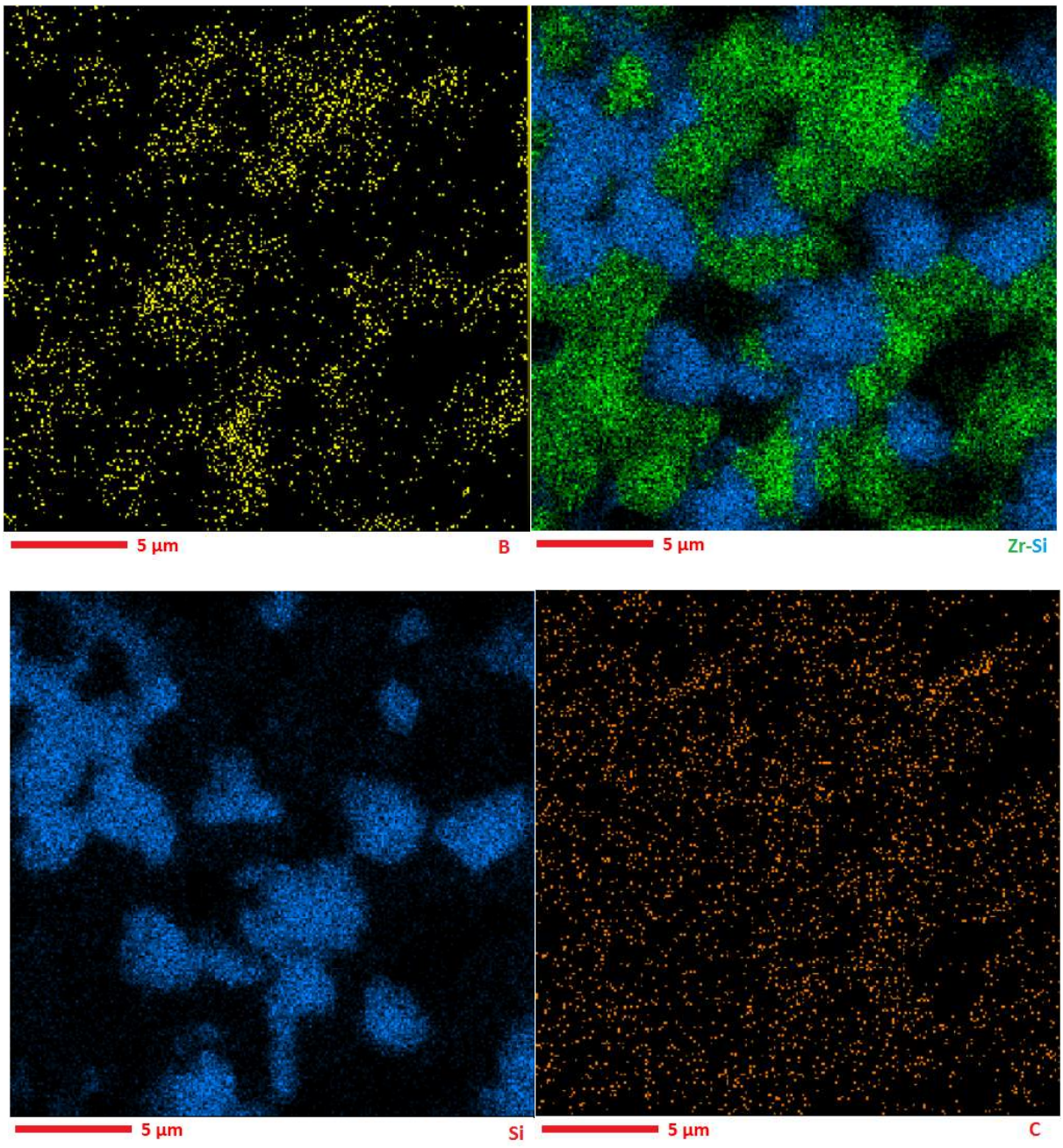

Continue Fig. 2. Map analysis of ZrB_2-30SiC-8HfB_2 SPSed at the condition of 1800, 9 min, 30 MPa

3.2. Oxidation behavior

Figure 3 shows the variation of weight change due to oxidation ($W_{C\text{-}O}$%) of samples versus the volume fraction of HfB_2 in all test durations. As it can be clearly seen, increased HfB_2 content leads to reduced $W_{C\text{-}O}$ percentage or in other words, higher oxidation resistance. Better understanding the oxidation behavior, cross-sectional SEM micrographs of the sample oxidized

for 20 hrs in 1400°C are presented in Figure 4. EDS line scan and X-ray map analyses of the mentioned samples are also presented in Figures 5 to 9.

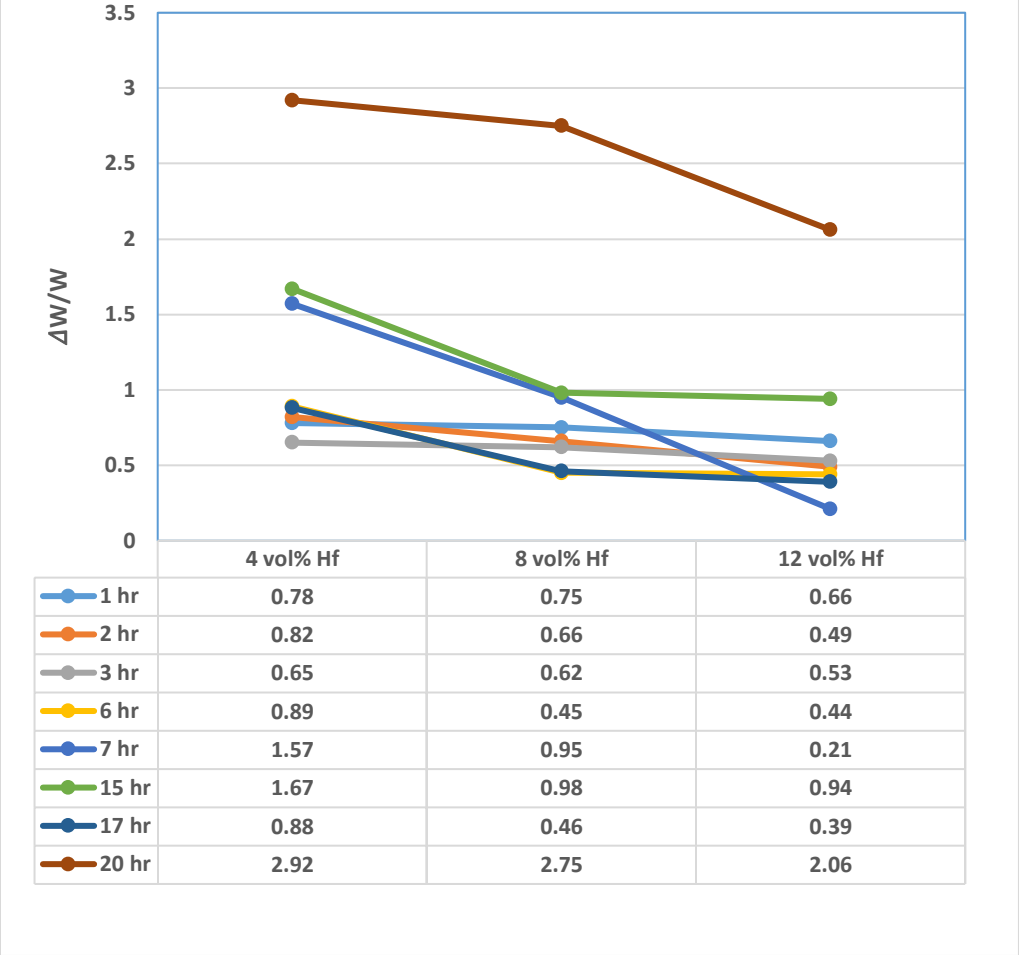

	4 vol% Hf	8 vol% Hf	12 vol% Hf
1 hr	0.78	0.75	0.66
2 hr	0.82	0.66	0.49
3 hr	0.65	0.62	0.53
6 hr	0.89	0.45	0.44
7 hr	1.57	0.95	0.21
15 hr	1.67	0.98	0.94
17 hr	0.88	0.46	0.39
20 hr	2.92	2.75	2.06

Fig. 3. $\Delta W_{C\text{-}O}\%$ of samples versus the volume fraction of HfB_2 in all test durations

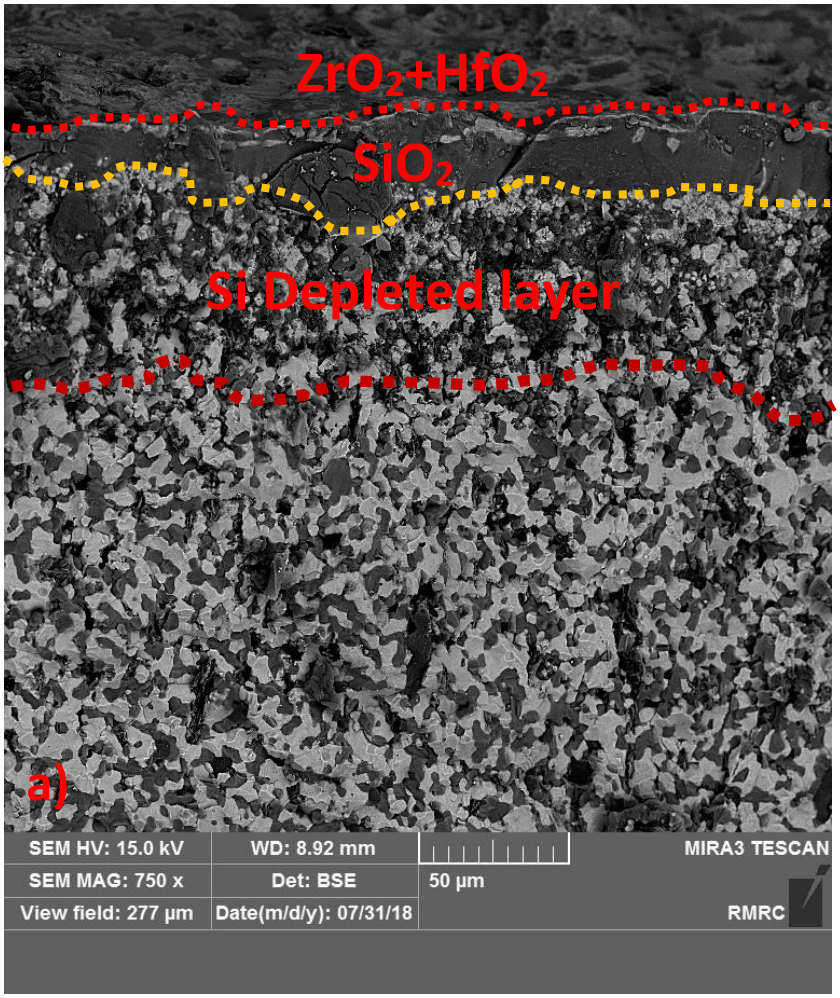

Fig. 4. SEM images of of ZrB_2-30SiC containing a) 4, b) 8 and c) 12 vol% HfB_2, after 20 hrs oxidation at 1400 °C

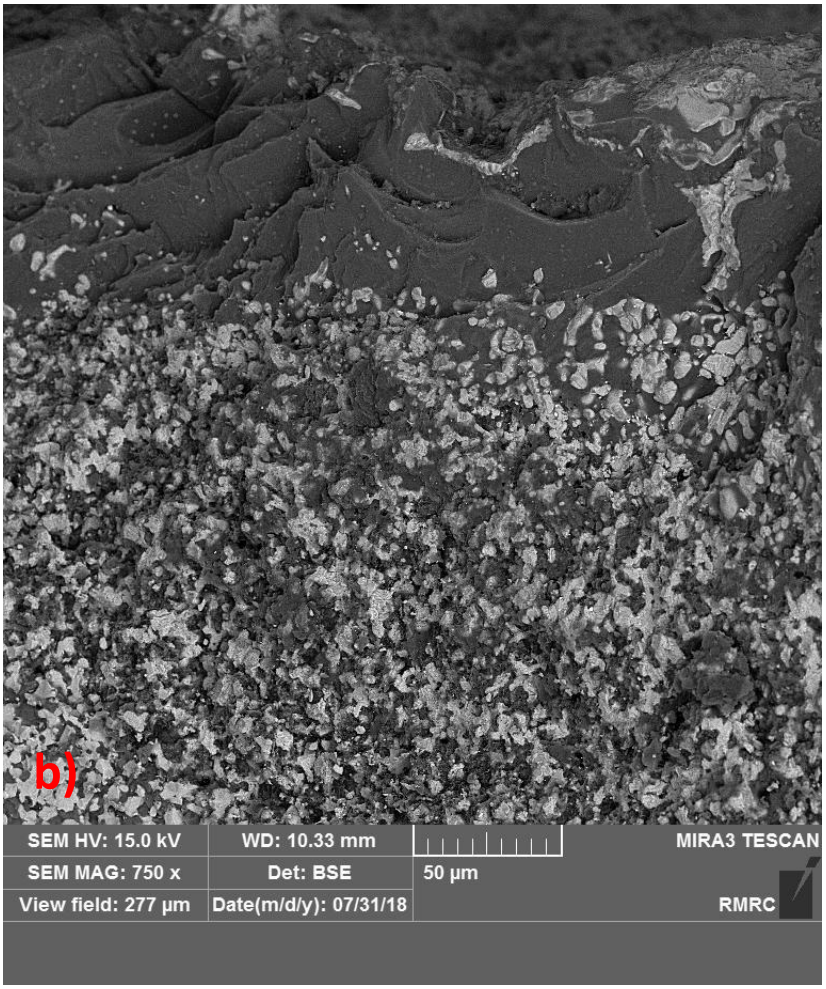

Continoue Fig. 4. SEM images of of ZrB_2-30SiC containing a) 4, b) 8 and c) 12 vol% HfB_2, after 20 hrs oxidation at 1400 °C

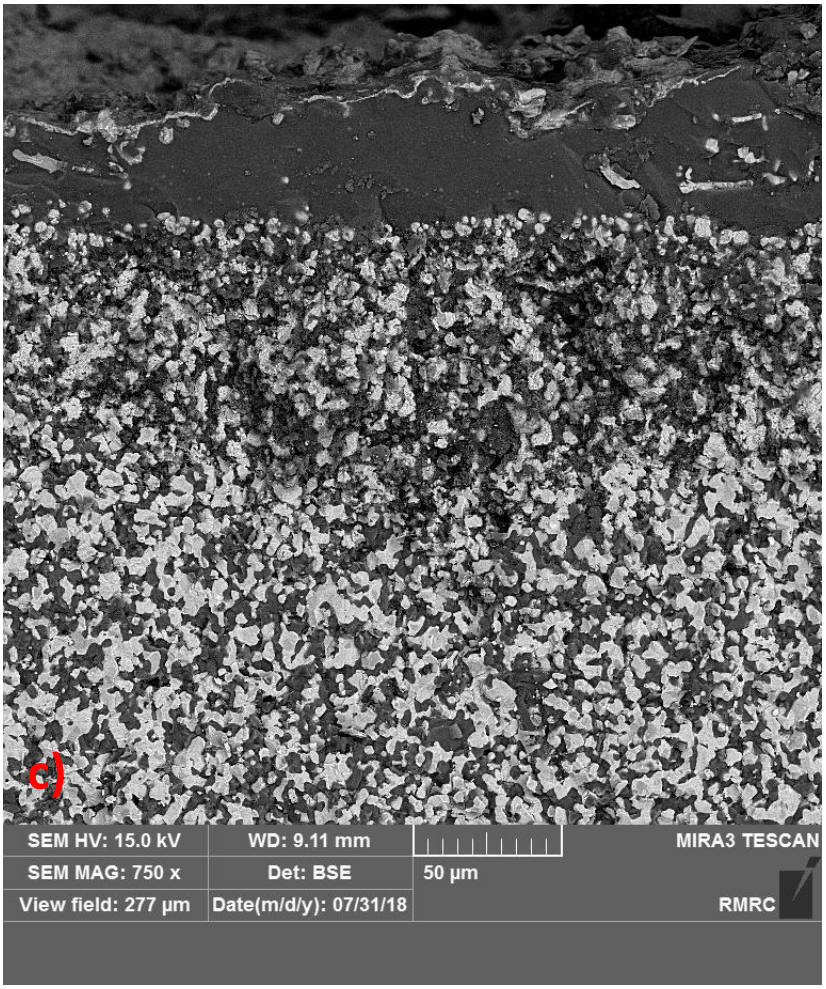

Continoue Fig. 4. SEM images of of ZrB_2-30SiC containing a) 4, b) 8 and c) 12 vol% HfB_2, after 20 hrs oxidation at 1400 °C

As it can be clearly seen in Figure 4, the polished cross-section of the samples reveals four distinct layers including very thin surface layer (white), dark and dense layer, dark and porous layer and the uninfluenced substrate (original microstructure of the composite). Based on the X-ray maps and EDS line scans (Figures 5-9), high concentration of Zr and O atoms in the first layer confirms the formation of ZrO2 on the surface of the samples. High concentrations of silicon and oxygen atoms accompanied with low concentration of carbon atoms indicate the formation of SiO2 on the second layer (dense and dark region). The third layer can be considered as silicon-depleted layer, as no traces of Si, O and Zr are detected.

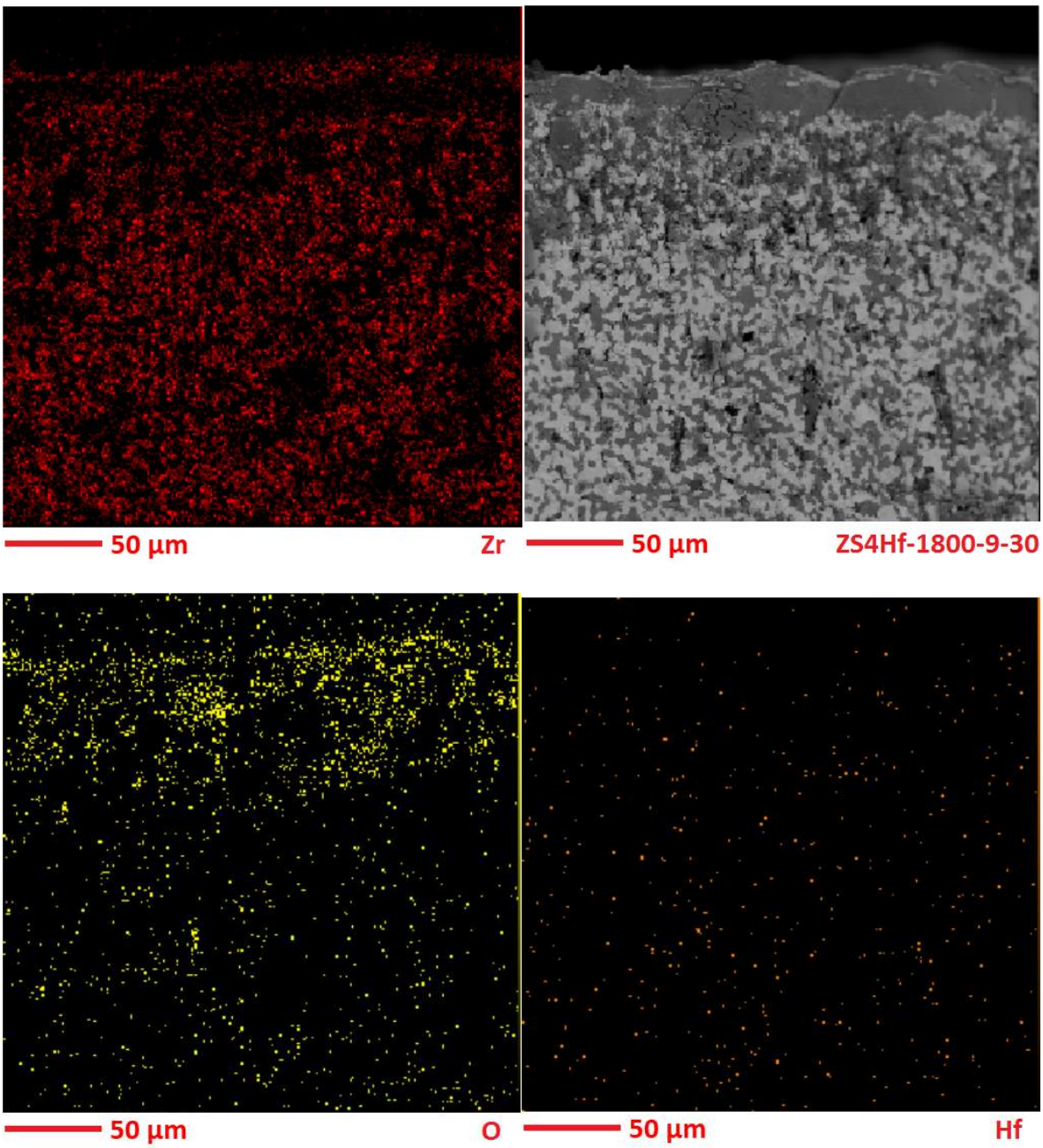

Fig. 5. Map analysis of ZrB_2-30SiC-4HfB_2 SPSed at the condition of 1800, 9 min, 30 MPa after oxidation for 20 hrs at 1400 °C

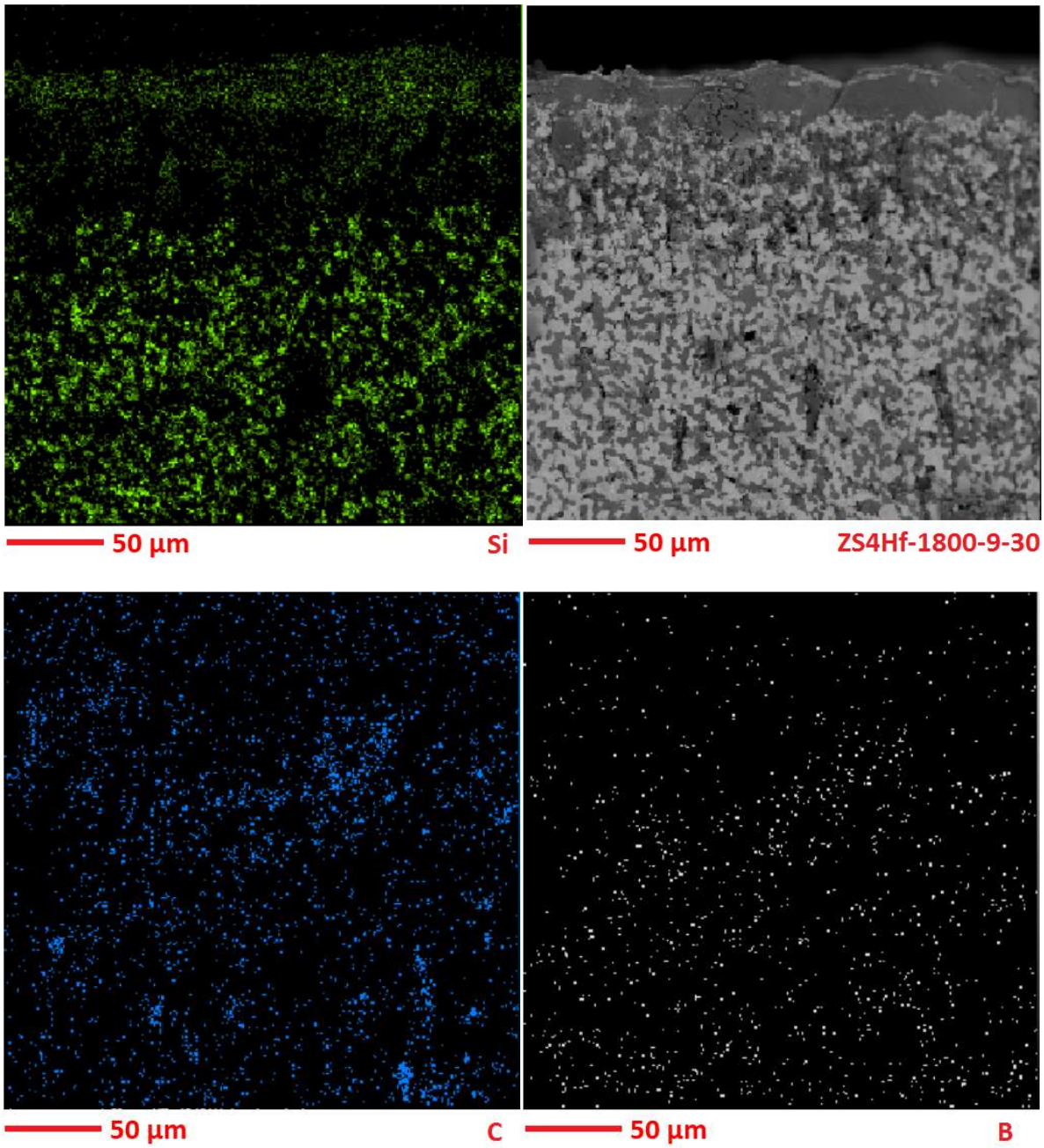

Continue Fig. 5. Map analysis of ZrB_2-30SiC-4HfB_2 SPSed at the condition of 1800, 9 min, 30 MPa after oxidation for 20 hrs at 1400 °C

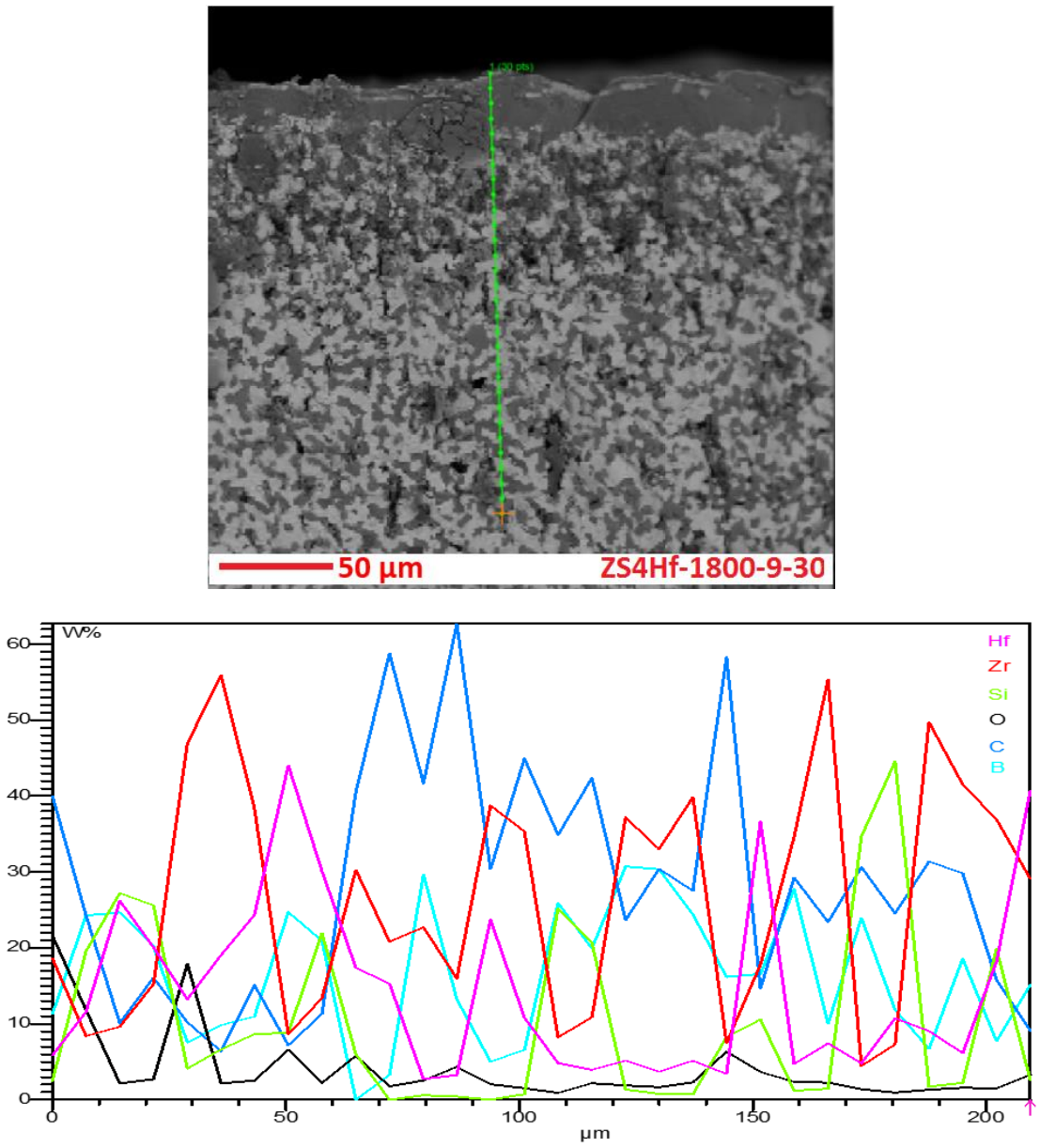

Fig. 6. Line analysis of ZrB_2-30SiC-4HfB_2 SPSed at the condition of 1800, 9 min, 30 MPa after oxidation for 20 hrs at 1400 °C

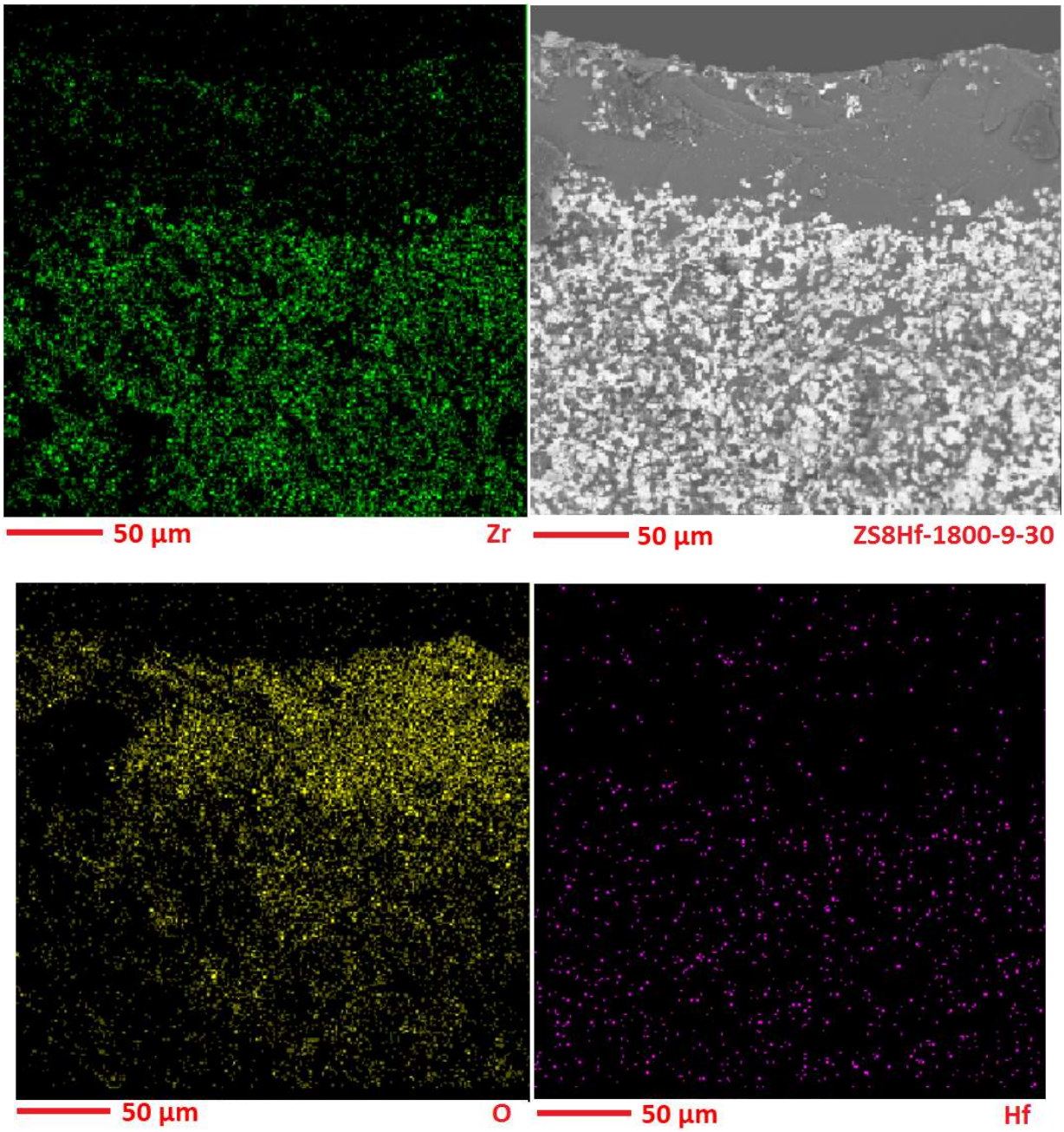

Fig. 7. Map analysis of ZrB_2-30SiC-8HfB_2 SPSed at the condition of 1800, 9 min, 30 MPa after oxidation for 20 hrs at 1400 °C

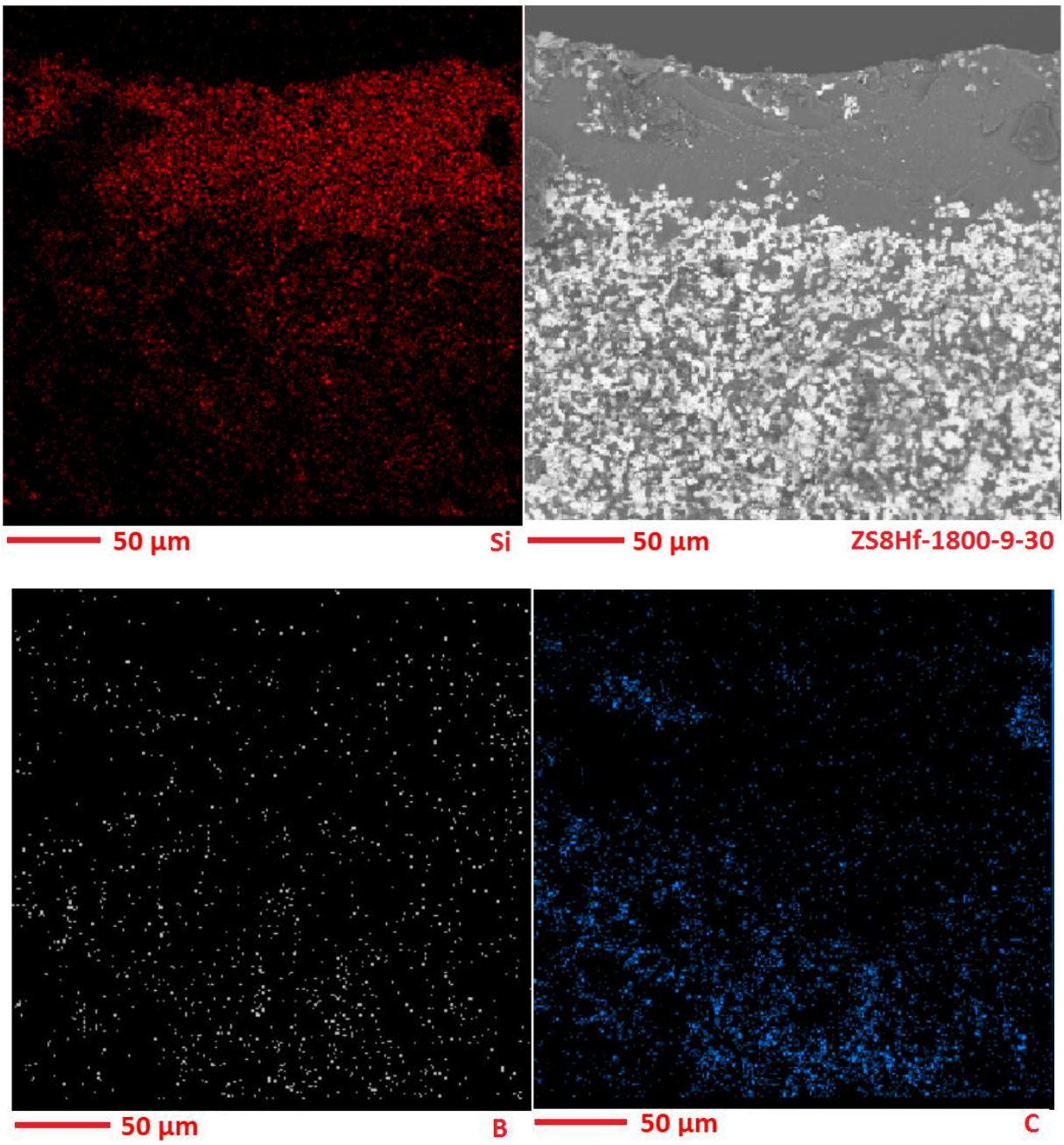

Continue Fig. 7. Map analysis of ZrB_2-30SiC-8HfB_2 SPSed at the condition of 1800, 9 min, 30 MPa after oxidation for 20 hrs at 1400 °C

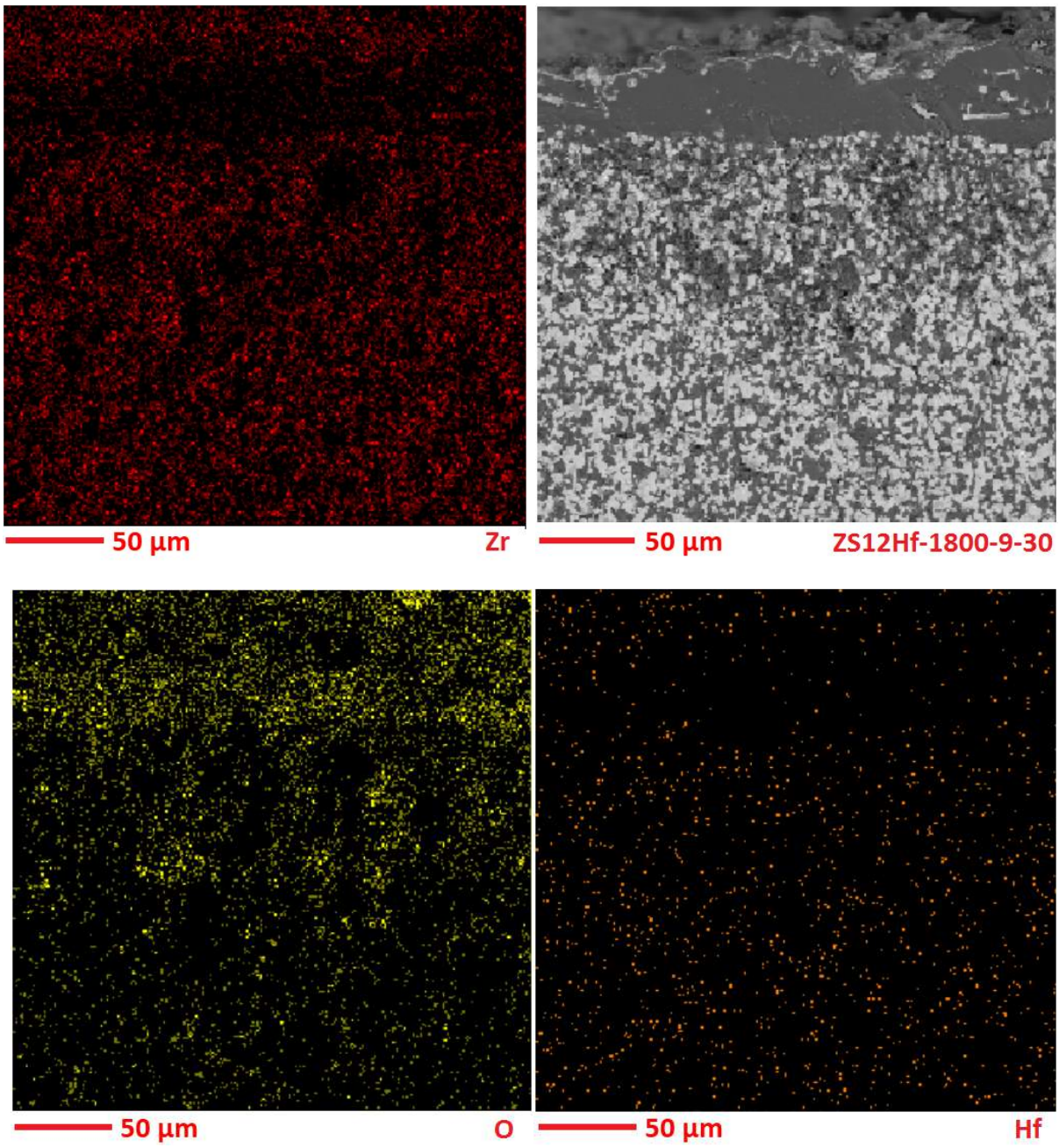

Fig. 8. Map analysis of ZrB_2-30SiC-12HfB_2 SPSed at the condition of 1800, 9 min, 30 MPa after oxidation for 20 hrs at 1400 °C

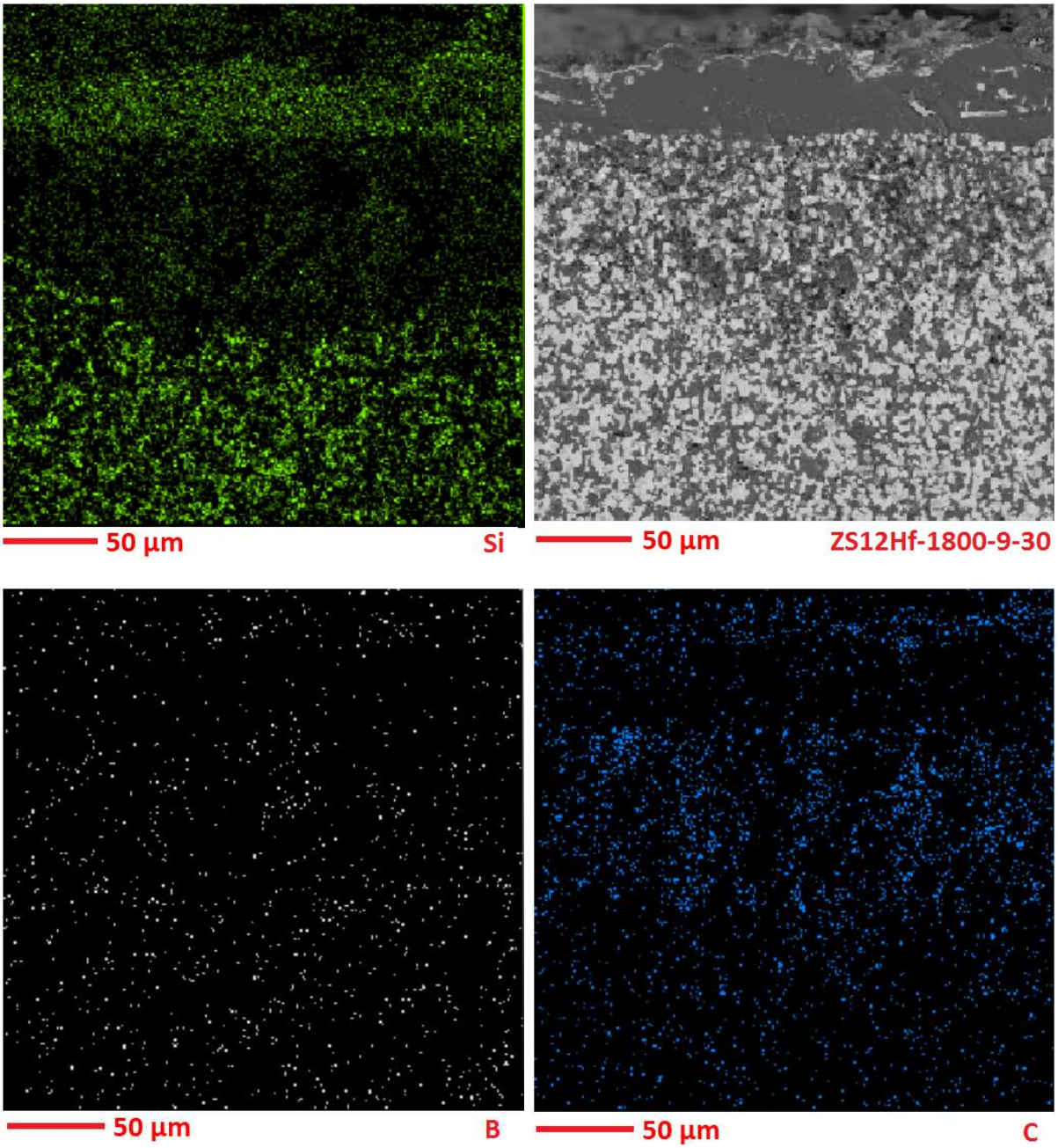

Continue Fig. 8. Map analysis of ZrB_2-30SiC-12HfB_2 SPSed at the condition of 1800, 9 min, 30 MPa after oxidation for 20 hrs at 1400 °C

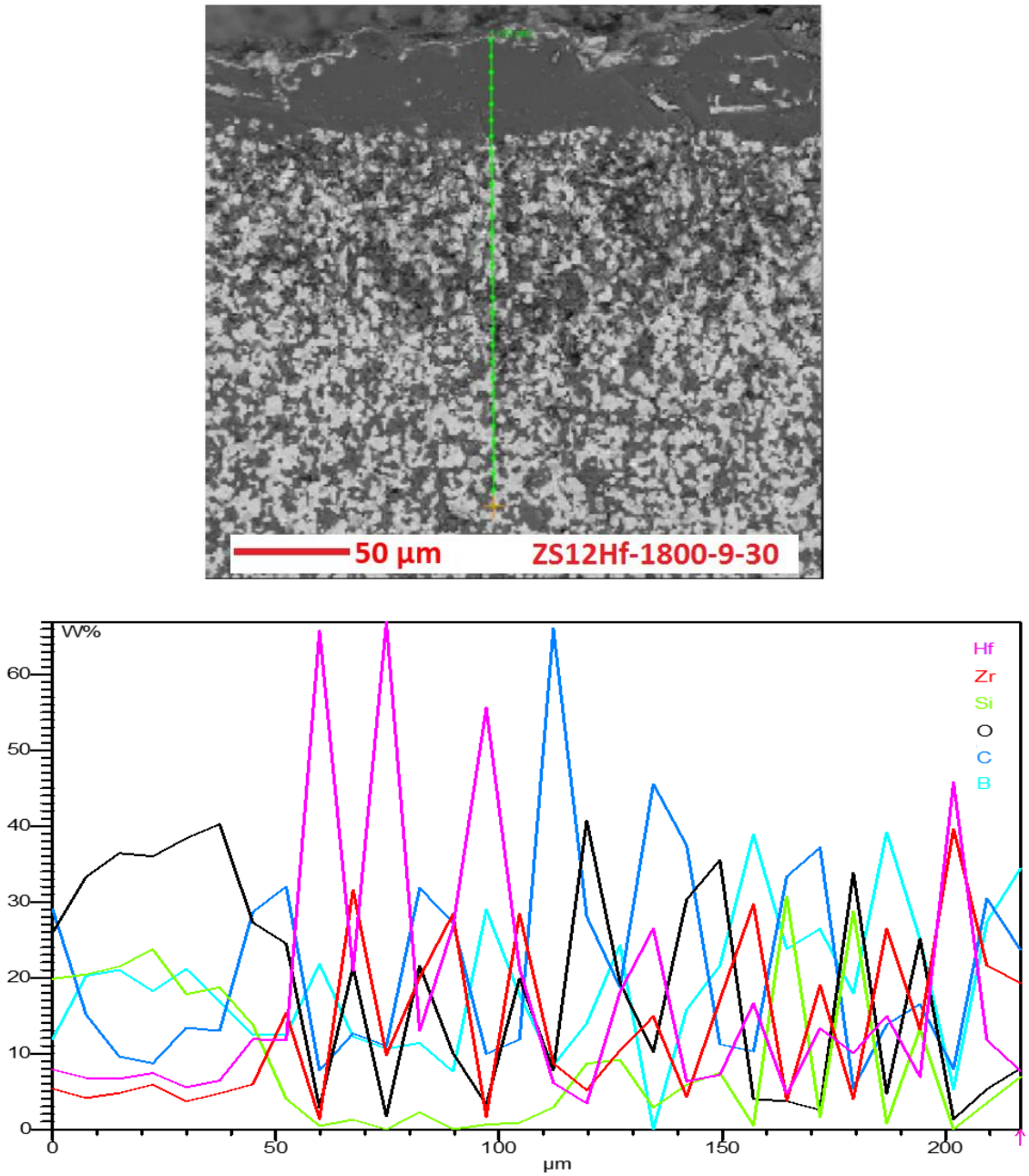

Fig. 9. Map analysis of ZrB_2-30SiC-12HfB_2 SPSed at the condition of 1800, 9 min, 30 MPa after oxidation for 20 hrs at 1400 °C

Tables 2 and 3 present the average thickness of the mentioned layers, based on SEM micrographs and chemical analyses (Figures 4 to 9). The oxidation of ZrB2, SiC and HfB2 as the main components of the composite can be conducted through the following chemical reactions [1-3]:

$$ZrB_2 + \frac{5}{2}O_2 \Rightarrow ZrO_2 + B_2O_3 \qquad (2)$$

$$HfB_2 + \frac{5}{2}O_2 \Rightarrow HfO_2 + B_2O_3 \qquad (3)$$

$$SiC + \frac{3}{2}O_2 \Rightarrow SiO_2 + CO \qquad (4)$$

Actually, the formation of SiO2 layer can result in the migration of silicon atoms toward the surface and consequently, silicon-depleted sublayer. Anyway, SiO2 may form a highly adhesive glassy layer on the surface (2nd layer) and increase the oxidation resistance of the composite, mainly due to interrupted atomic diffusion paths. On the other hand, although higher amounts of HfB2 can lead to thinner SiO2 layer, as the thickness of Si-depleted layers simultaneously decreases; improved oxidation resistance of the composite is expected.

It has been reported that SiC can increase the oxidation resistance of ZrB2 and HfB2-based ceramics. Such a positive role can be attributed to the formation of glassy borosilicate layer (B2O3-SiO2) instead of B2O3, which has higher viscosity and thermal stability, as well as lower vapor pressure. Therefore, borosilicate layers not only decrease the diffusion rate of oxygen atoms (as the main oxidation controlling parameter) due to higher viscosity, but also tolerate higher temperatures (thermal stability) which prolong their protection role. Besides its viscosity, molten borosilicate layer provides a favorable wettability with both ZrO2 and HfO2 compounds which promotes the filling of surface porosities and consequently, prevents oxygen atoms from diffusion in porosities. Such a mechanism is known as the main oxidation controlling parameter of HfB2-SiC composites up to 1400°C. Although similar mechanism can be proposed for ZrB2-SiC composites, the oxidation resistance of ZrB2 is lower than HfB2, due to volume changes accompanied with the phase transformation of ZrO2, as well as higher diffusion coefficient of oxygen atoms in ZrO2 compared with HfO2 [2]. Such a phenomenon can be clearly seen in X-ray maps of figures 5, 7 and 8.

The oxidation behaviors of hot-pressed ZrB2-20 vol.% SiC and HfB2-20 vol.% SiC composites were investigated by Mallik et al [2], through non-isothermal TGA up to 1300°C, 1, 24 and 100 hrs isothermal TGA at 1200 and 1300 °C and full-cycle (24 cycles, each one for 1 hr) oxidation test (including heating up to 1300 °C and cooling down in air), and similar results were reported.

It also worth to note that thickening the SiO2 layer leads to more scattered distribution of ZrO2 grains (lower fraction of ZrO2 grains), which is clearly emphasized from X-ray maps and indicates the consumption of Zr atoms, and consequently results in weaker oxidation resistance.

Oxidation mechanism

Figure 10 shows the weight change of sample 17 vs time, after oxidation at 1400 °C, which indicates higher oxidation rate (higher weight change) when holding time is increased. It can be attributed to increased diffusion of oxygen atoms into the surface of the samples and thickening the oxide layers and oxidation-affected zones. The following function can be fitted to the curves presented in Figure 10:

$$\left[(\Delta w / s)\right]^{n} = 65.3t \qquad (5)$$

Where, n=2.24 here. It has been confirmed that when n>2.00, the oxidation process is parabolically controlled by diffusion or in other word, the diffusion rate of O atoms plays the key role in oxidation behavior of the composite[18].

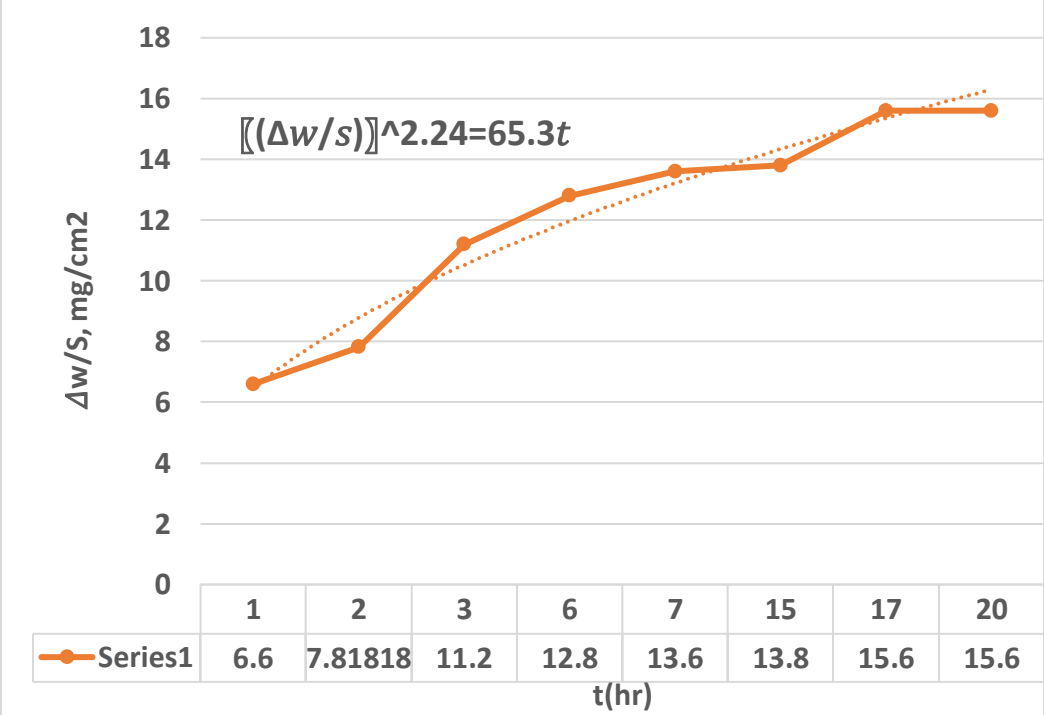

Fig. 10. The weight change of samples vs time, after oxidation at 1400 °C

Conclusions

Results indicated that the presence of HfB2 can promote the formation of HfO2, which reduces the diffusion rate of oxygen atoms and consequently, results in improved oxidation resistance of the composite.

It was also revealed that the oxidation products are formed as three distinct layers, including a very thin ZrO2 surface layer, a ZrO2+SiO2 middle layer and the inner Si-depleted layer. It was also indicated that the middle layer itself consisted of two sublayers: relatively pure SiO2 sublayer and a semi-composite sublayer of ZrO2 grains dispersed in SiO2 matrix. Finally, it was concluded that thicker semi-composite layer would result in better oxidation resistance of hf-doped ZrB2-30 vol.% SiC composites.

Reference

[1] Ping Hu a,*, Wang Guolin b, Zhi Wang, Oxidation mechanism and resistance of ZrB2–SiC composites, Corrosion Science 51 (2009) 2724–2732

[2] Manab Mallik, K.K. Ray, R. Mitra, Oxidation behavior of hot pressed ZrB2–SiC and HfB2–SiC composites, Journal of the European Ceramic Society 31 (2011) 199–215

[3] Peter A. Williams a, Ridwan Sakidja, John H. Perepezko, Patrick Ritt, Oxidation of ZrB2–SiC ultra-high temperature composites over a wide range
of SiC content, Journal of the European Ceramic Society 32 (2012) 3875–3883

[4] Z. Balak, Mohammad Zakeri, Application of Taguchi L_{32} orthogonal design to optimize flexural strength of ZrB_2-based composites prepared by spark plasma sintering, Int. Journal of Refractory Metals and Hard Materials 55 (2016) 58–67

[5] Z. Balak, M. Zakeri, Effect of HfB_2 on microstructure and mechanical properties of ZrB_2–SiC-based composites, Int. Journal of Refractory Metals and Hard Materials 54 (2016) 127–137

[6] Zohre Balak, Mehdi Shahedi Asl, Mahdi Azizieh, Hosein Kafashan, Raziye Hayati, Effect of different additives and open porosity on fracture toughness of ZrB_2–SiC-based composites prepared by SPS, Ceramics International 43 (2017) 2209–2220

[7] Pouya Vaziri, zohre Balak, Improved mechanical properties of ZrB_2-30 vol% SiC using Zirconium carbide additive, *International Journal of Refractory Metals and Hard Materials* https://doi.org/10.1016/j.ijrmhm.2019.05.004

[8] Keyvan Kavakeb, Zohre Balak, Hosein Kafashan, Densification and flexural strength of ZrB2–30vol% SiC with different amount of HfB2, *International Journal of Refractory Metals and Hard Materials,* https://doi.org/10.1016/j.ijrmhm.2019.104971

[9] Zohre Balak, Shrinkage, hardness and fracture toughness of ternary ZrB_2-SiC-HfB_2 composite with different amount of HfB_2, Materials chemistry and physics

[10] M. Shahedi Asl, A statistical approach towards processing optimization of ZrB_2-SiC-graphite nanocomposites. Part I: Relative density, Ceramics International, 44 (2018) 6935.
[11] Rozbe Eatemadi, Zohre Balak, Investigating the effect of SPS parameters on densification and fracture toughness of ZrB_2-SiC nanocomposite ,Cer. Int. 45 (2019)4763.
[12] M Shahedi Asl, Microstructure, hardness and fracture toughness of spark plasma sintered ZrB_2-SiC-C_f composites, Ceramics International 43 (2017) 15047.
[13] Sadegh Karimirad, Zohre Balak, Characteristics of spark plasma sintered ZrB_2-SiC-SCFs composites, Ceramics International, 45 (2019) 6275.
[14] Laura Silvestronia, Elena Landia, Katarzyna Bejtkab, Angelica Chiodonib, Diletta Sciti, Oxidation behavior and kinetics of ZrB2containing SiC chopped fibers, Journal of the European Ceramic Society 35 (2015) 4377–4387

[15] D. Gao, Y. Zhang, C. Xu, Y. Song, X. Shi, Oxidation kinetics of hot-pressedZrB2–SiC ceramic matrix composites, Ceram. Int. 39 (2013) 3113–3119.

[16] F. Peng, G. Van Laningham, R.F. Speyer, Thermogravimetric analysis of the oxi-dation resistance of ZrB2–SiC and ZrB2–SiC–TaB2-based compositions in the1500–1900◦C range, J. Mater. Res. 26 (2011) 96–107

[17] Hua Jinn, Songhe Meng, Xinghong Zhang, Qingxuan Zeng, Jiahong Niu, Effects of oxygen partial pressure on the oxidation of ZrB2–SiC–graphite composites at1800 C, Ceramics International42(2016)6480–6486

[18] Hua Jin, Songhe Meng, Xinghong Zhang, Qingxuan Zeng, Jiahong Niu, Effects of oxidation temperature, time, and ambient pressure on the oxidation of ZrB2–SiC–graphite composites in atomic oxygen, Journal of the European Ceramic Society 36 (2016) 1855–1861

Figures

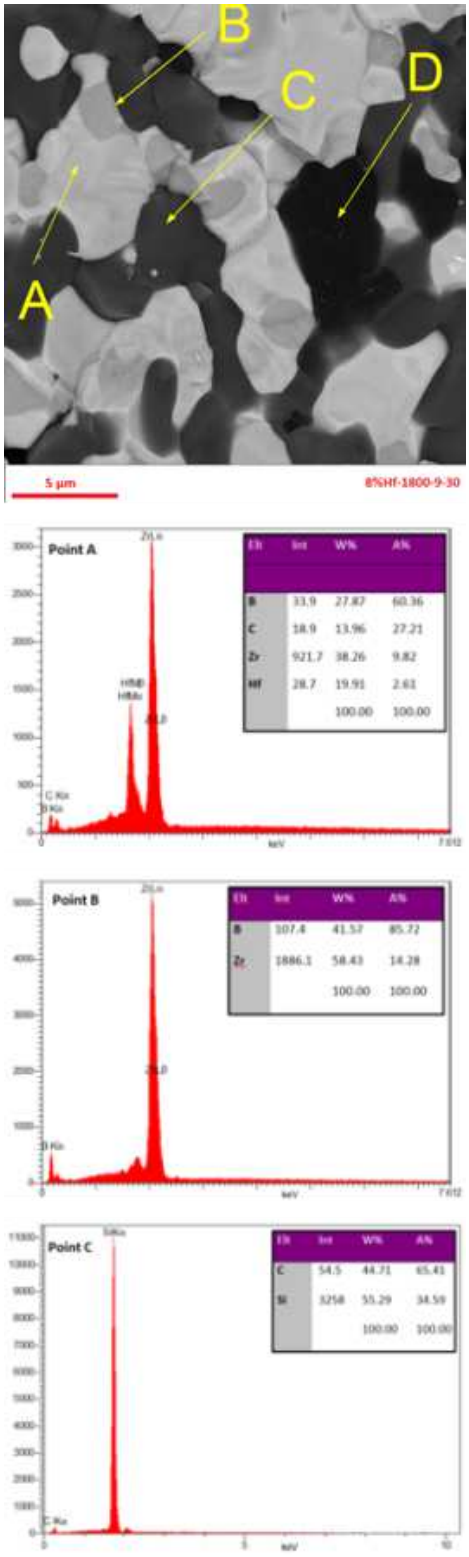

Figure 1

Point analysis of ZrB2-30SiC-8HfB2 SPSed at the condition of 1800, 9 min, 30 MPa

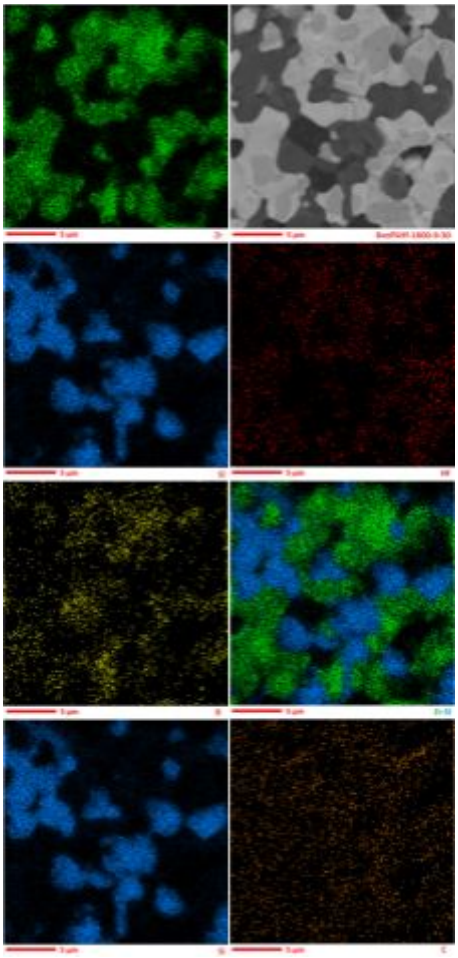

Figure 2

Map analysis of ZrB2-30SiC-8HfB2 SPSed at the condition of 1800, 9 min, 30 MPa

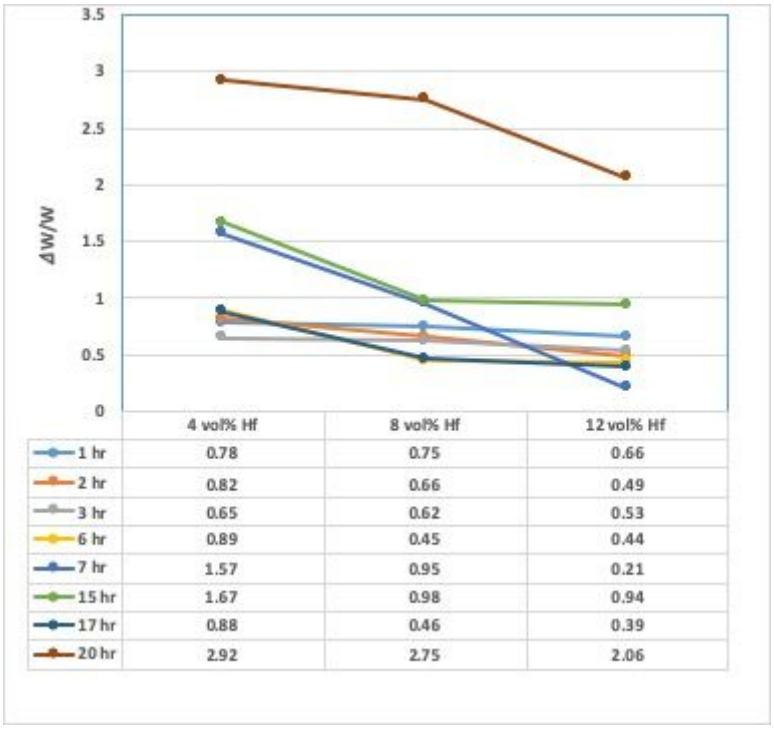

	4 vol% Hf	8 vol% Hf	12 vol% Hf
1 hr	0.78	0.75	0.66
2 hr	0.82	0.66	0.49
3 hr	0.65	0.62	0.53
6 hr	0.89	0.45	0.44
7 hr	1.57	0.95	0.21
15 hr	1.67	0.98	0.94
17 hr	0.88	0.46	0.39
20 hr	2.92	2.75	2.06

Figure 3

WC-O% of samples versus the volume fraction of HfB2 in all test durations

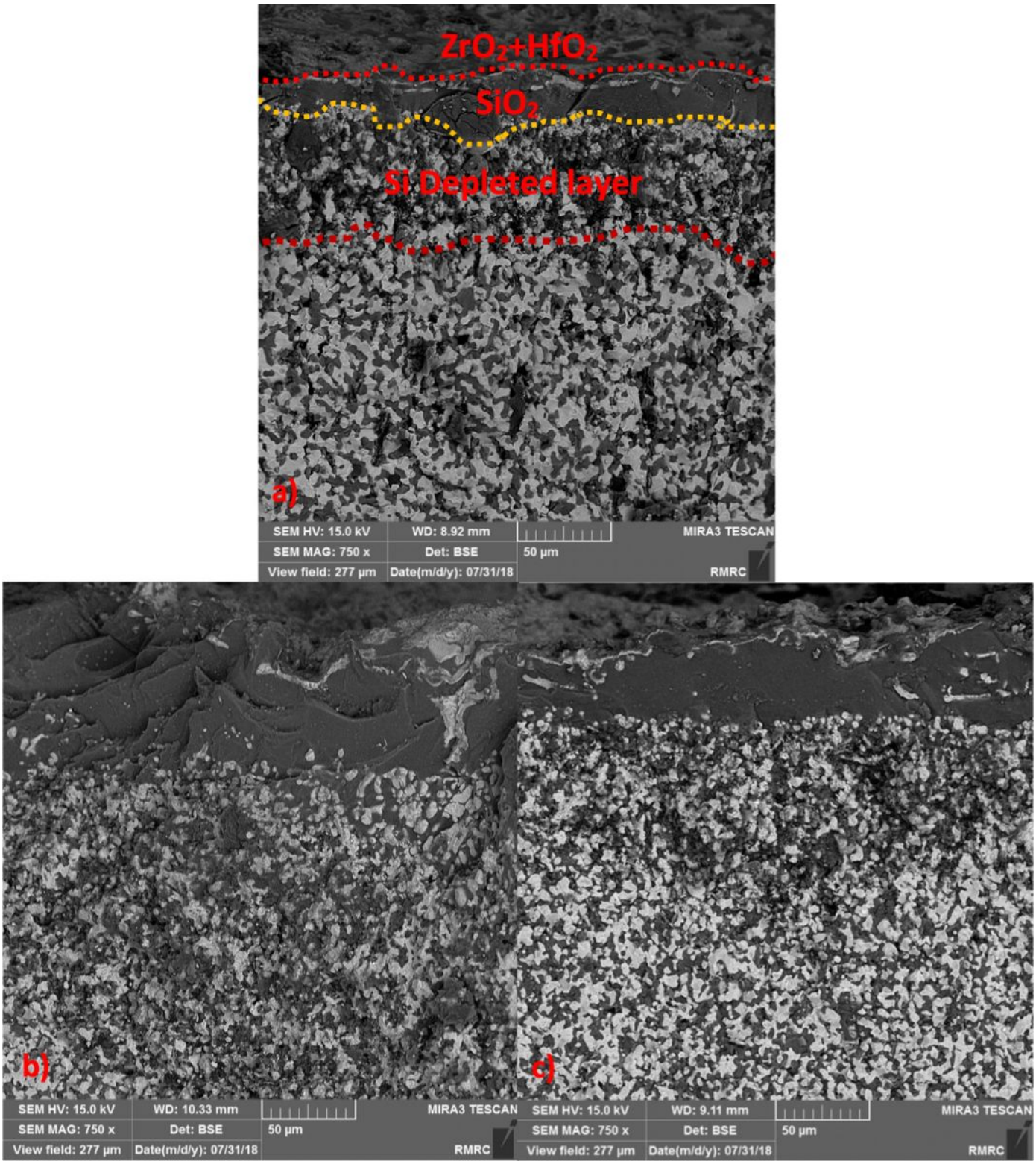

Figure 4

SEM images of of ZrB2-30SiC containing a) 4, b) 8 and c) 12 vol% HfB2, after 20 hrs oxidation at 1400 °C

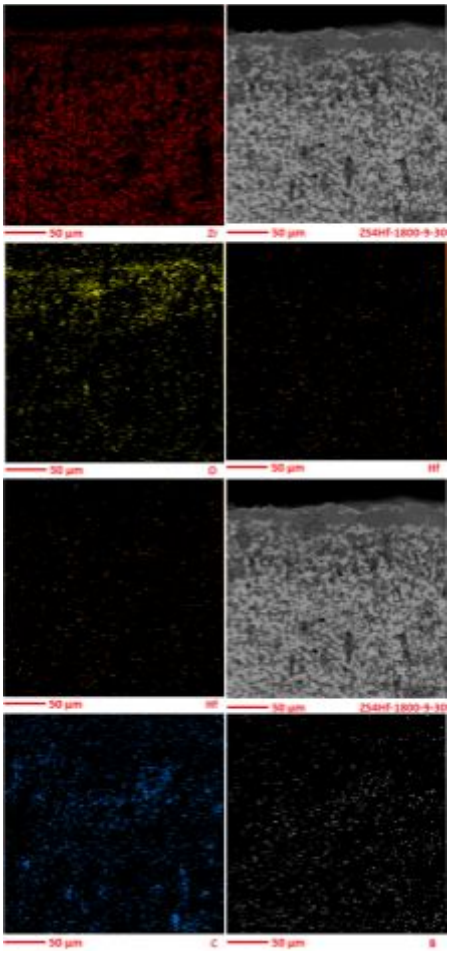

Figure 5

Map analysis of ZrB2-30SiC-4HfB2 SPSed at the condition of 1800, 9 min, 30 MPa after oxidation for 20 hrs at 1400 °C

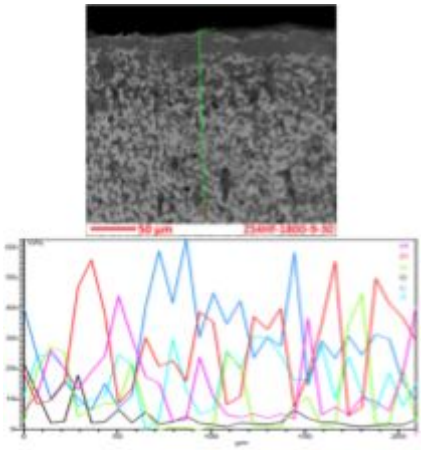

Figure 6

Line analysis of ZrB2-30SiC-4HfB2 SPSed at the condition of 1800, 9 min, 30 MPa after oxidation for 20 hrs at 1400 °C

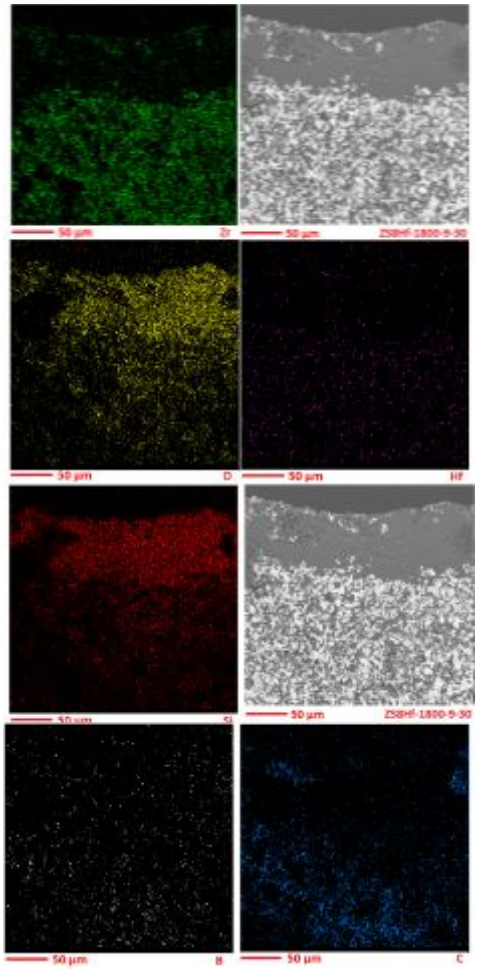

Figure 7

Map analysis of ZrB2-30SiC-8HfB2 SPSed at the condition of 1800, 9 min, 30 MPa after oxidation for 20 hrs at 1400 °C

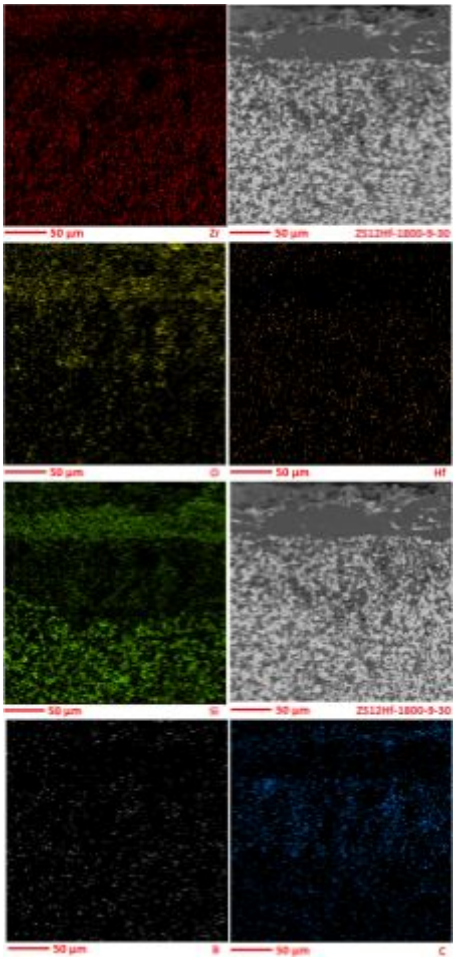

Figure 8

Map analysis of ZrB2-30SiC-12HfB2 SPSed at the condition of 1800, 9 min, 30 MPa after oxidation for 20 hrs at 1400 °C

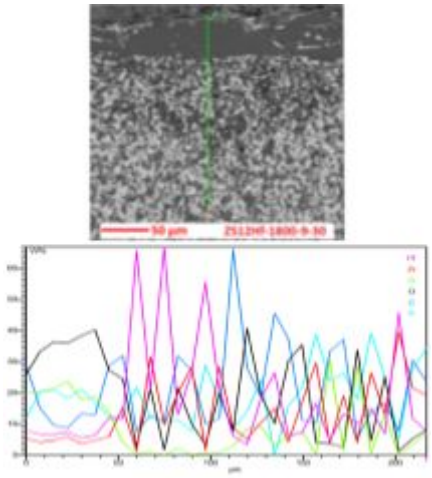

Figure 9

Map analysis of ZrB2-30SiC-12HfB2 SPSed at the condition of 1800, 9 min, 30 MPa after oxidation for 20 hrs at 1400 °C

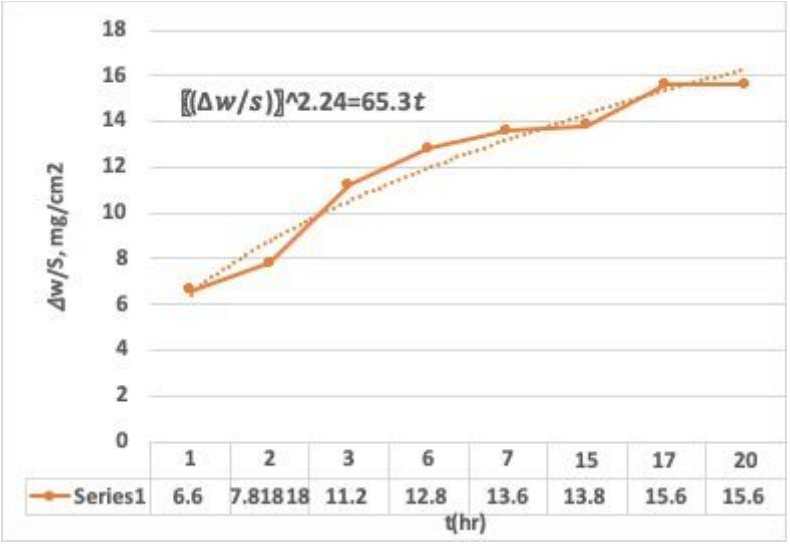

Figure 10

The weight change of samples vs time, after oxidation at 1400 °C